


Cite this: *J. Mater. Chem. B*, 2025,
13, 13781

Hydrolytic degradation of PEG-based thiol–norbornene hydrogels enables multi-modal controlled release

Nathan H. Dimmitt and Chien-Chi Lin *

Poly(ethylene glycol) (PEG) hydrogels crosslinked by orthogonal thiol–norbornene click chemistry have emerged as an ideal platform for tissue engineering and drug delivery applications due to their rapid crosslinking kinetics and excellent biocompatibility. Norbornene-functionalized PEG (PEGNB) is routinely synthesized through the Steglich esterification of 5-norbornene-2-carboxylic acid with hydroxyl-terminated PEG. When crosslinked with thiol-bearing macromers, PEGNB hydrogels undergo slow hydrolytic degradation due to hydrolysis of ester bonds connecting a PEG backbone and a NB moiety. In prior work, we replaced the pungent and nauseous 5-norbornene-2-carboxylic acid with odorless carbic anhydride (CA) for synthesizing PEG–norbornene-carboxylate (PEGNB_{CA}), a new macromer that could be readily photo-crosslinked into thiol–norbornene hydrogels with faster hydrolytic degradation than the PEGNB counterparts. In this contribution, we employed a modular approach to tune the hydrolytic degradation of PEGNB_{CA} hydrogels over days to months. We first demonstrated the diverse crosslinking of PEGNB_{CA} hydrogels using either photopolymerization or enzymatic crosslinking. We characterized the hydrolytic degradation of these hydrogels under different solution pH values and temperatures. *Via* adjusting crosslinker functionality and the ratio of fast-degrading PEGNB_{CA} to slow-degrading PEGNB, tunable hydrolytic degradation of PEGNB_{CA} hydrogels was achieved from under 2 days to over 3 months. Finally, we designed the highly tunable PEGNB_{CA} hydrogels with varying mesh sizes, degradation rates, and covalent tethering of degradable linkers to afford long-term controlled release of model drugs.

Received 26th June 2025,
Accepted 22nd September 2025

DOI: 10.1039/d5tb01524c

rsc.li/materials-b

Introduction

Poly(ethylene glycol) (PEG)-based hydrogels are widely used in biomedical applications owing to their excellent biocompatibility and tunable tissue-like elasticity.¹ One of the PEG-based hydrogels widely adapted for biomedical applications is chain-polymerized PEG-diacrylate (PEGDA).^{1,2} Despite its lengthy synthesis steps that require meticulous control of all reaction conditions, especially the slow addition of acryloyl chloride, PEGDA has found numerous biomedical applications as it is adaptable for various chemical modifications. However, chain-growth polymerizations yield heterogeneous polymer networks and prolonged radical propagation that can damage the encapsulated biologics.¹ Furthermore, while the ester bond connecting PEG and acrylate is hydrolytically labile, the high-molecular-weight polyacrylate kinetic chains in the chain-polymerized networks are hydrophobic and non-degradable, rendering the PEGDA hydrogels with extremely slow to no *in vivo* clearance.¹

Structurally, chain-polymerized PEGDA hydrogels are mesoporous, with a ‘mesh size’ of the order of a few tens of nanometers.³ As such, the mobility of encapsulated macromolecules (*e.g.*, large proteins and cells) is restricted unless the hydrogels are designed to undergo local or global degradation. In this regard, Hubbell *et al.* pioneered hydrolytically degradable PEG-based hydrogels *via* copolymerizing poly(lactic acid) (PLA) with PEG, followed by acrylation of the linear PLA–PEG–PLA copolymers.⁴ The resulting acryl–PLA–PEG–PLA–acryl macromers were crosslinked into covalent hydrogels with a tunable degradation rate by adjusting the molecular weight of the PLA blocks.⁵

PEG-based hydrogels can also be crosslinked through step-growth polymerizations, such as the Michael addition reactions between multi-arm PEG derivatives (*e.g.*, (meth)acrylate, vinyl-sulfone, and maleimide) and thiol-bearing crosslinkers.^{2,6–10} For example, the Hubbell group engineered PEG-based hydrogels by crosslinking multi-arm PEG–acrylate with bis-cysteine-containing peptide linkers labile to matrix metalloproteinases (MMPs).^{6,8} These hydrogels demonstrated high biocompatibility and enzymatic degradability and were used as carriers to release a

Weldon School of Biomedical Engineering, Purdue University, West Lafayette, IN, USA. E-mail: lin711@purdue.edu; Tel: +1(965) 495-7791



recombinant human bone morphogenic protein (rhBMP2) for treating calvarial defects in rats. Metters and Hubbell demonstrated the predictable hydrolytic degradation of thioether-ester bonds in the Michael-type thiol-acrylate hydrogels,⁵ enabling sustained release of human growth hormone (hGH).⁷ The crosslinking of thiol-acrylate hydrogels was commonly accelerated by using base catalyst triethanolamine (TEOA)⁷ or initiated by light and a photoinitiator.^{11,12} While the network properties of Michael-type hydrogels can be pre-engineered, their crosslinking was not tunable after mixing the mutually reactive macromers. In contrast, radical-mediated step-growth photopolymerization offers unique advantages in creating a well-defined hydrogel network with mild and on-demand tunable gelation.¹³ For example, the Anseth group synthesized multi-arm PEG-norbornene (PEGNB) for forming thiol-norbornene photopolymerized hydrogels as a versatile synthetic extracellular matrix.¹⁴ Our group later characterized and modeled the hydrolytic degradability of PEGNB hydrogels under physiological conditions.¹⁵ We also engineered PEGNB hydrogels resistant to hydrolysis by replacing the ester group on 4-arm PEGNB with an amide bond.¹⁶ The Kloxin group explored PEGNB hydrogels for protein release, but no attempt was made to control hydrogel degradation.¹⁷

While PEGNB has become increasingly used in hydrogel crosslinking, its organic synthesis was laborious and tedious and required stringent containment efforts. Conventionally, PEGNB was synthesized by Steglich esterification between the hydroxyl moiety on the PEG macromer and the acid group on the pungent 5-norbornene-2-carboxylic acid using anhydrous dichloromethane (DCM) as the solvent.¹⁴ In this reaction, dicyclohexylcarbodiimide (DCC) is needed for activating 5-norbornene-2-carboxylic acid into norbornene anhydride, whereas dimethylaminopyridine (DMAP) is used as a nucleophilic catalyst for the esterification with norbornene anhydride. Efforts to improve the degree of norbornene substitution on PEG include: (1) azeotropic distillation of bond water by reflux in anhydrous toluene, followed by rotary evaporation to remove toluene; (2) blanking the reaction vessel with inert gas; (3) multiple additions of reactants; and (4) small batch reactions (<5 g).¹⁸ Notably, hydrolytic degradation of PEGNB-crosslinked thiol-norbornene hydrogels was achieved without conjugating an additional hydrolytically labile linker, owing to the hydrolytic susceptibility of ester on PEGNB.¹⁵

To improve the efficiency of PEGNB synthesis, our lab developed an alternative synthesis route that replaced the pungent 5-norbornene-2-carboxylic acid with odorless carbic anhydride (CA) and used DMAP as the only catalyst.¹⁹ Compared with conventional synthesis, the new CA method produced a similar norbornene substitution but with reduced synthesis time (2 days) as no PEG distillation and norbornene acid activation steps were required. This new macromer, PEGNB-carboxylate (PEGNB_{CA}), can be readily crosslinked into hydrogels *via* a thiol-norbornene photo-click reaction^{19,20} or a norbornene-tetrazine inverse electron-demand Diels-Alder (iEDDA) click reaction.^{21,22} Like PEGNB, the new PEGNB_{CA} could also be crosslinkable by an enzyme-initiated thiol-norbornene click reaction.²³

The use of enzymes to initiate hydrogel crosslinking may be more advantageous for some biomedical applications due to the specificity and tunability of the catalytic reaction.^{24,25} However, enzyme-initiated PEGNB_{CA} hydrogel crosslinking has not been demonstrated. Nonetheless, we found that hydrogels crosslinked by PEGNB_{CA} underwent accelerated hydrolytic degradation compared to those crosslinked by PEGNB. Specifically, the hydrolysis rate was approximately 5 times higher in PEGNB_{CA} gels than in PEGNB gels with similar crosslinking density.¹⁹

We reason that the accelerated hydrolytic degradation of PEGNB_{CA} hydrogels could be leveraged to produce hydrogels with tunable degradation for controlled release applications. In this contribution, we investigated the gelation kinetics of ester-based PEGNB and PEGNB_{CA} hydrogels with different thiol crosslinkers. From there, we characterized the subsequent hydrogel properties, including degradation over time under different conditions (*e.g.*, pH of the buffer and incubation temperature). The hydrolytic degradation rate was further controlled *via* modular blending of PEGNB and PEGNB_{CA} crosslinked by different thiol crosslinkers. Finally, we leveraged the higher degradability of the ester bond on PEGNB_{CA} for multimodal release, including crosslinking gels with varying mesh size and degradation rate, and tethering of thiol-bearing drugs onto PEGNB_{CA} for their degradation-controlled release.

Materials and methods

Materials

8-Arm hydroxyl-terminal PEG (PEG-OH, 10 kDa and 20 kDa) and 8-arm thiol-terminal PEG (PEG8SH, 10 kDa) were purchased from JenKem Technology. 4-Arm thiol-terminal PEG (PEG4SH, 10 kDa) was purchased from Laysan Bio Inc. Dithiothreitol (DTT) was purchased from Fisher Scientific. Pyridine, anhydrous dichloromethane (DCM), and 1-(3-dimethylamino-propyl)3-ethylcarbodiimide hydrochloride (EDC) were obtained from Thermo Scientific. 5-Norbornene-2-carboxylic acid, tetrahydrofuran (THF), 4-dimethylaminopyridine (DMAP), *N,N'*-dicyclohexylcarbodiimide (DCC), and lithium phenyl-2,4,6-trimethylbenzoylphosphinate (LAP) were purchased from Sigma-Aldrich. Carbic anhydride was purchased from Acros Organics. Phosphate buffered saline tablets were purchased from Fisher Scientific and prepared according to the manufacturer's recommendation. Fluorescein PEG thiol (MW 3400) was purchased from NANOCS. Bovine serum albumin was purchased from Fisher (Cytiva HyClone™ BSA). The Bradford reagent was purchased from Bio-Rad (Quick Start™ Bradford Protein Assay).

Macromer synthesis and purification

Synthesis of PEGNB. Before synthesis, PEG-OH was dried *in vacuo* under desiccant for at least 1 day. 8-Arm PEGNB was synthesized according to a previously established protocol.^{15,18} Briefly, dried PEG-OH was dissolved in toluene and then heated to 115 °C connected to a Dean stark trap and condenser column to remove any excess water contained in the PEG polymer.



After several hours of reflux, toluene was dried out using a rotary evaporator. PEG was solvated in dichloromethane (DCM) and purged with N₂ gas. In a separate reaction vessel, norbornene acid (5 eq. relative to hydroxyl on PEG-OH) reacted with 2.5 eq. DCC in anhydrous DCM for at least 1 hour, followed by vacuum filtration using size 52 filter paper to remove the urea byproduct. The filtrate was transferred to an addition funnel where it was added dropwise to the reaction vessel containing dried PEG-OH in DCM. DMAP (1 eq.) and pyridine (5 eq.) were added to the reaction vessel and purged with N₂ gas. After the overnight reaction, a second addition of activated norbornene acid was added and allowed to react for an additional 24 hours. Synthesized PEGNB was precipitated using diethyl ether and dried *in vacuo* with a desiccant for overnight, then dissolved in water and dialyzed for three days using a 3.5 kDa MWCO dialysis tube.

Synthesis of PEGNB_{CA}. PEGNB_{CA} was synthesized following a previous report.¹⁹ Briefly, PEG-OH was dried *in vacuo*, dissolved in tetrahydrofuran (THF), and heated to 60 °C, followed by addition of carbic anhydride (5 eq.) and DMAP (1 eq.).¹⁹ After 24 hours of reaction, an additional 5 eq. of carbic anhydride and 1 eq. DMAP were added to the reaction vessel for another overnight reaction. PEGNB_{CA} was dialyzed in ethanol for 1 day and in water for 2 days using 3.5 kDa MWCO dialysis tubing. Both PEGNB_{CA} and PEGNB were frozen at -80 °C for several hours and placed on a Labconco freeze-dryer. Norbornene substitution of the synthesized polymers was determined using ¹H NMR spectroscopy with deuterium oxide as the solvent comparing the protons associated with the alkene group on the norbornene to the protons on the PEG backbone.

Photocrosslinking of PEGNB or PEGNB_{CA} via thiol-norbornene chemistry

PEGNB or PEGNB_{CA} was crosslinked with DTT, PEG4SH, or PEG8SH at a stoichiometric ratio (*i.e.*, $R([\text{SH}]/[\text{NB}] = 1)$) using 2 mM LAP and 365 nm light at 20 mW cm⁻² intensity unless specified otherwise. A stoichiometric ratio was chosen to ensure the highest degree of step-growth crosslinking, since previous studies have shown that the off-stoichiometric ratio of thiol to norbornene led to dangling polymer chains that did not contribute to network crosslinking.^{15,16,18} To prepare hydrogels, 45 μL of hydrogel precursor solution was deposited between two glass slides treated with hydrophobic windshield coating (*i.e.*, Rainaway) separated by 1 mm Teflon spacers. The hydrogel precursor solution contained within the slide was placed under a 365 nm light bar lamp for 2 minutes. Prior to measuring elastic and loss moduli (G' and G''), the hydrogels were incubated in pH 7.4 PBS at 37 °C for at least one hour to ensure equilibrium swelling. Strain sweep (0.1 to 5.0% strain) tests were conducted using a Bohlin CVO digital rheometer fitted with an 8 mm diameter parallel geometry plate. The oscillating frequency was fixed at 1 Hz, which falls within the linear viscoelastic region (LVR). The gelation point was defined as the time required for the G' to surpass the G'' during *in situ* photorheometry testing, which was conducted using an Anton-Paar MCR102 rheometer equipped with a UV-curing system fitted with a 25 mm parallel geometry plate. During the test,

200 μL of hydrogel precursor solution was deposited on the rheometer stage, and the plate was lowered to 0.300 mm in height. Time sweep test was then started with a fixed strain at 1% and frequency at 1 Hz over a five-minute period. After 30 seconds, the light (Omnigene S2000, fitted with a 365 nm light filter at 5 mW cm⁻²) was turned on for two minutes.

Enzymatic crosslinking of PEGNB_{CA} using HRP with thiol-based crosslinkers

Enzymatic crosslinking of PEGNB_{CA} was conducted using horse radish peroxidase (HRP) with or without hydrogen peroxide (H₂O₂), which mediates thiol radical formation and then subsequently crosslinks to the vinyl bond on the norbornene functional group.^{23,26} Unless specified otherwise, enzymatically crosslinked PEGNB_{CA} hydrogels were fabricated using 20 U mL⁻¹ HRP and 100 μM of H₂O₂. For enzymatic crosslinking without H₂O₂, the concentration of HRP was increased to 1 kU mL⁻¹. For *in situ* rheology, the Anton Paar MCR102 rheometer was fitted with a peltier platform and a 25 mm parallel plate head with temperature set at 37 °C. The hydrogel precursor solution was deposited on the stage followed by lowering the plate head to 0.300 mm in height. The time sweep test was then started with a fixed strain at 1% and frequency at 1 Hz over a 20-minute period with measurements being taken every 2 seconds. For hydrogel fabrication, the hydrogel precursor solution was placed between two glass slides treated with hydrophobic coating and separated by 1 mm Teflon spacers. The slides containing the hydrogel precursor solution were placed in a sealed container along with a Petri dish of water to increase the humidity to prevent drying. The sealed container was placed in an incubator set at 37 °C and allowed to react for 1 hour. Afterwards, hydrogels were swelled in pH 7.4 PBS and incubated at 37 °C unless specified otherwise.

Effect of temperature and pH on hydrolytic degradation of PEGNB or PEGNB_{CA} hydrogels

PBS was prepared using tablets according to the manufacturer's recommendation. Without any addition of a base or an acid, the pH value after preparation was 7.4, which was measured using a pH meter (Mettler Toledo). Using 1 N NaOH, the pH of the PBS was adjusted to 12 and by using 1 N HCl, the pH of the PBS was adjusted to 3. 5 wt% PEGNB_{CA} or PEGNB hydrogels crosslinked with PEG4SH at $R = 1$ with 2 mM LAP were fabricated through 365 nm exposure at 20 mW cm⁻² for 2 minutes. Subsequently, the hydrogels were incubated in PBS with pH values of 3, 7.4, or 12 at 37 °C. Strain sweep tests were conducted at corresponding time points to track the changes in G' occurring over time. For temperature study, 5 wt% PEGNB_{CA} crosslinked with PEG4SH at $R = 1$ was utilized and swelled in pH 7.4 PBS at either 37 °C using an incubator or kept at room temperature (*i.e.*, 25 °C). The G' of these hydrogels was measured at corresponding time points.

Effect of crosslinker functionality and polymer content on hydrolytic degradation

To assess the effect of macromer functionality and polymer content, PEGNB_{CA} hydrogels were crosslinked at either 5 wt%,



10 wt%, or 20 wt% with either DTT, PEG4SH, or PEG8SH at $R = 1$. The hydrogels were crosslinked using 365 nm light at 20 mW cm⁻² using 2 mM LAP. Post-crosslinking, the hydrogels were swelled in pH 7.4 PBS at 37 °C. The G' was measured at corresponding time points of the different hydrogel formulations using the strain sweep test. The G' values obtained over time were normalized to the G' value obtained after 1 hour incubation in pH 7.4 PBS at 37 °C. The normalized G' values were then fitted to exponential decay kinetics using Prism 10 software with an initial value set at 1 and the final plateau value fixed at 0 to indicate complete degradation. From here, the $k_{\text{hydrolysis}}$ value was derived from the fitting as well as the degradation half-times ($t_{1/2}$).

In addition to G' , we assessed the hydrolytic degradation by measuring changes in the mass swelling ratio (Q) overtime. For this study, the volume of the initial hydrogel was increased to 100 μL and was prepared using water instead of PBS except for hydrogels crosslinked with DTT since gelation was not possible using water. Post-gelation, the hydrogels were dried *in vacuo* for at least 1 day. Once dried, the hydrogels were weighed using an analytical balance (Mettler Toledo) to obtain dried weight 1 (W_1). The hydrogels were then swelled in distilled water overnight. The following day the hydrogels were dried *in vacuo* for at least one day and were subsequently weighed to obtain dried weight 2 (W_2). The hydrogels were then swelled in pH 7.4 PBS at 37 °C and were weighed at corresponding timepoints to obtain the swollen mass (W_s). The equation below was utilized to obtain the mass swelling ratio.

$$Q = \frac{W_s - W_2}{W_2} \quad (1.1)$$

The mass swelling ratios obtained over time were normalized to the initial mass swelling ratio, which was obtained after 1 hour incubation at 37 °C in pH 7.4 PBS. The values were then fitted using exponential growth using Prism 10 software with a fixed initial value of 1.

Tuning the hydrolytic degradation through PEGNB_{CA}/PEGNB blended hydrogels

To tune the hydrolytic degradation of PEG thiol–norbornene crosslinked hydrogels, we blended PEGNB_{CA} with PEGNB at different ratios. The total macromer concentration was fixed at 10 wt%. The different ratios (wt% PEGNB_{CA}/wt% PEGNB) tested were 4/6, 6/4, 8/2, and 9/1. The different ratios of macromers were crosslinked with either DTT, PEG4SH, or PEG8SH. Hydrogels were stored under physiological conditions (*i.e.*, pH 7.4 PBS at 37 °C) for up to 150 days. During this time, changes in G' were tracked. The G' values were normalized to the initial values, which were obtained after 1 hour of swelling after gel fabrication. The normalized G' values were fitted using exponential decay fitting, where the $k_{\text{hydrolysis}}$ and degradation half-time ($t_{1/2}$) were obtained.¹⁹

PEGNB_{CA} based hydrogels for multi-modal release

For release studies, 5 wt% PEGNB_{CA} (8-arm, 10 kDa) was crosslinked with PEG8SH at a stoichiometric ratio unless

otherwise noted. To evaluate pure diffusion-controlled release, three proteins of different sizes were chosen as model cargos: lysozyme (~14 kDa), bovine serum albumin (BSA, ~65 kDa), and bovine gamma globulin (BGG, ~150 kDa). All proteins were encapsulated in the hydrogels at a fixed concentration of 20 mg mL⁻¹. Protein-encapsulated hydrogels (50 μL) were incubated in 2 mL PBS at 37 °C. At predetermined time points, 50 μL of solutions were collected and replaced with an equal volume of protein-free PBS. Protein quantification was performed using the protein assay kit (Bio-Rad Quick Start™) according to the manufacturer's recommendation without modification. The accumulated release amount was calculated by quantifying the concentration and amount of protein at the time of collection plus the amounts that were sampled in previous time points.

Large size fluorescein isothiocyanate-dextran (FITC-Dextran, 70 kDa or 150 kDa) was utilized for degradation-controlled release studies as these large molecules would be trapped in the hydrogels unless significant hydrogel degradation occurred. Unless specified otherwise, FITC-dextran was encapsulated within the PEGNB_{CA} or PEGNB crosslinked thiol–norbornene hydrogel at a concentration of 0.5 mg mL⁻¹. The hydrogel precursor solution containing FITC-dextran was pipetted in 100 μL increments into 4 separate 2 mL centrifuge tubes. The tubes were then exposed to 365 nm light for 2 minutes to induce gelation. Subsequently, the hydrogels were incubated with pH 7.4 PBS at 37 °C. 200 μL aliquots were taken from the 2 mL tubes at different time points and placed in a 96-well black polystyrene plate, where the fluorescent intensity was measured (485 nm excitation and 528 nm emission) using a microplate reader (Biotek Synergy HT). After measuring, the aliquots were pipetted back into the 2 mL tubes. To recover the fluorescence probe for calculating cumulative release, equivalent hydrogel formulations were degraded at 80 °C (pH 12 for PEGNB hydrogels). If the hydrogel underwent complete degradation, the fluorescence intensities were normalized to this value. For fluorescently labeled dextran, values were normalized to PEGNB_{CA} control post-degradation, since the accelerated degradation reduced the fluorescence intensity of FITC-dextran.

PEG conjugated with fluorescein containing thiol (FITC-PEG-SH, 3.4 kDa) was tethered onto norbornene pendants on PEGNB or PEGNB_{CA}. The macromer content of PEGNB or PEGNB_{CA} was fixed at 10 wt% and was crosslinked with PEG8SH at $R = 0.8$. The hydrogel precursor solution also contained 2.5 mg mL⁻¹ of PEG-fluorescein-SH and 2 mM LAP. The hydrogel precursor solution was pipetted in 50 μL increments into 2 mL centrifuge tubes and was crosslinked through 365 nm light exposure at 20 mW cm⁻² for 2 minutes. The hydrogels were then incubated with 1 mL of PBS for 1 hour to remove any unconjugated FITC-PEG-SH. To measure conjugation efficiency, the PBS was removed and fluorescence intensity was measured and normalized to the unconjugated fluorescent dye at the same concentration. The hydrogels were incubated with pH 7.4 PBS at 37 °C. Fluorescence was measured by pipetting 200 μL aliquots into a 96-well black



polystyrene plate. The fluorescence intensity was measured using a microplate reader. The aliquots were pipetted back into the 2 mL centrifuge tubes. The fluorescence intensity was normalized to controls that underwent accelerated degradation.

Statistics/software

All data are presented as the mean with error bars being the standard error of the mean (SEM). For two conditions, the unpaired *t*-test was performed with statistical significance having $p < 0.05$. For two or more conditions, one-way or two-way ANOVA was performed using the Tukey *post-hoc* test. Statistical significance between conditions is represented with $p < 0.05$ (* $p < 0.05$, ** $p < 0.01$, *** $p < 0.001$, and **** $p < 0.0001$). All statistical analysis and data fitting were conducted with GraphPad Prism 10. Initial constraints were placed on the model including Y_0 was fixed to 1 and the plateau value was set to equal 0. The equation utilized on Prism software is shown below.

$$Y = (Y_0 - \text{Plateau}) \times e^{-k_{\text{hydrolysis}} \times x} + \text{Plateau}$$

where Y is the normalized G' value, x is the time in terms of days, and $k_{\text{hydrolysis}}$ is the rate of change in normalized G' based upon hydrolytic degradation in units of inverse days (d^{-1}). All studies were performed with at least 3 replicates. Furthermore, all chemical structures were drawn using Chemdraw.

Results and discussion

Photopolymerization of PEGNB and PEGNB_{CA} hydrogels

Norbornene-functionalized PEG can be synthesized by conjugating norbornene acid (NB) or carbic anhydride (CA) onto hydroxyl-terminal PEG, yielding PEGNB or PEGNB_{CA}, respectively (Fig. 1(A)). Previous work has shown that both PEGNB and PEGNB_{CA} could be crosslinked into thiol–norbornene hydrogels using DTT as a crosslinker under 365 nm light with LAP as the photoinitiator.¹⁹ In this study, we achieved high norbornene substitutions (>90%) for 8-arm PEGNB_{CA} with two molecular weights, 10 kDa and 20 kDa (Fig. S1). We varied hydrogel network connectivity using thiol-based crosslinkers with different functionalities (f), including DTT ($f = 2$), PEG-tetra-thiol (PEG4SH, $f = 4$), and PEG-octa-thiol (PEG8SH, $f = 8$) (Fig. 1(B)). Thiol–norbornene photo-click gelation (Fig. 1(C)) was characterized using *in situ* photorheometry (Fig. 1(D) and (E)), with gel point defined as the time when the storage modulus (G') surpasses the loss modulus (G'') (Fig. S2) on the photorheometry plots. At a low LAP concentration of 2 mM and a low 365 nm light intensity of 2 mW cm^{-2} , gel points were reached in under ~11.3 s, 10.5 s, and 7 s for 20 kDa PEGNB gels were crosslinked with $f = 2, 4$, and 8, respectively (Fig. S2). For PEGNB_{CA}, the three gel points identified were faster for all three thiol-crosslinkers, at ~6.3 s, 9 s, and 3.5 s (Fig. S2). Decreasing LAP concentrations from 2 mM to 0.125 mM led to a slower gel point of ~35 s (Fig. 1(F)). The correlation between the LAP concentration and the gel point could be modeled through one-phase decay fitting, with R^2 greater than 0.95 for both PEGNB

and PEGNB_{CA}. Higher crosslinker functionality led to substantially stiffer hydrogels, with PEG8SH crosslinked gels reaching ~120 kPa for PEGNB and ~70 kPa for PEGNB_{CA} (Fig. 1(G)). Gelation of 10 kDa PEGNB_{CA} was equally efficient as that in the 20 kDa macromer, with gel points falling under 6 seconds for all three thiol crosslinkers (Fig. S3). However, hydrogels crosslinked by 10 kDa PEGNB_{CA} were significantly stiffer than those crosslinked by the 20 kDa counterpart (1.5-fold to 2-fold higher in G' . Fig. 1(H)), which was attributed to the higher norbornene molarity at the same macromer weight content (*i.e.*, 5 wt%).

The high efficiency of step-growth thiol–norbornene gelation was further affirmed by comparing the gel point of chain-growth gelation of PEGDA, which was 4-fold slower (*i.e.*, 20 seconds) using 2.2 mM LAP and a higher light intensity (365 nm light at 10 mW cm^{-2}).²⁷ Higher LAP concentrations generated higher radical concentrations at the onset of photocrosslinking, resulting in faster gelation.^{27,28} The effects of polymer functionality and molecular weights on hydrogel crosslinking density and stiffness have been described by the rubber elasticity theory, where the elastic modulus is proportional to polymer functionality and inversely proportional to the distance between crosslinks.^{29,30} However, we noticed that PEGNB_{CA} hydrogels consistently have significantly lower G' than the equivalent PEGNB hydrogels (Fig. 1(G)). Interestingly, PEGNB_{CA} hydrogels had similar or higher gel fractions and significantly higher mass swelling ratios compared with the equivalent PEGNB hydrogels (Fig. S4), indicating that the lower stiffness of PEGNB_{CA} hydrogels was not due to inefficient crosslinking but could be attributed to higher water absorbability due to the charged NB_{CA} moieties.³¹ Additionally, we found that photoinitiator LAP only impacted the crosslinking density and elastic moduli of PEGNB_{CA} hydrogels (crosslinked with PEG4SH) at concentrations lower than 0.5 mM (Fig. S5). LAP concentration beyond 0.5 mM (*ca.* 0.0147 wt%) resulted in no significant changes in G' , highlighting the efficient thiol–norbornene photocrosslinking of PEGNB_{CA} hydrogels.²⁸

Enzymatic crosslinking of PEGNB_{CA} hydrogels

While light and radical-mediated thiol–norbornene hydrogel crosslinking provides many benefits, this gelation mechanism cannot be readily adopted in the clinics for minimally invasive hydrogel delivery where the desired *in vivo* location is deeper than subcutaneous sites. Thus, developing light-independent gelation is essential for injectable and minimally invasive hydrogel delivery *in vivo*. To this end, we have shown that the thiol–norbornene click-reaction can be initiated by HRP in the presence or absence of exogenous H_2O_2 .^{23,26} Similar to the HRP-mediated thiol-crosslinking of PEGNB hydrogels, we found that PEGNB_{CA} could also undergo enzymatic crosslinking with the thiol-crosslinker (Fig. 2(A)).²⁶ Interestingly, gelation with PEGNB_{CA} was one order of magnitude faster than that with PEGNB at 05 kU mL^{-1} HRP and in the absence of H_2O_2 (gel points of 2.2 min and 18.5 min for PEGNB_{CA} and PEGNB, respectively. Fig. 2(B)). Unlike photocrosslinking, HRP-mediated gelation in the absence of exogenous H_2O_2 was slower to reach plateau moduli, with G' reaching ~1.2 kPa, ~3 kPa,



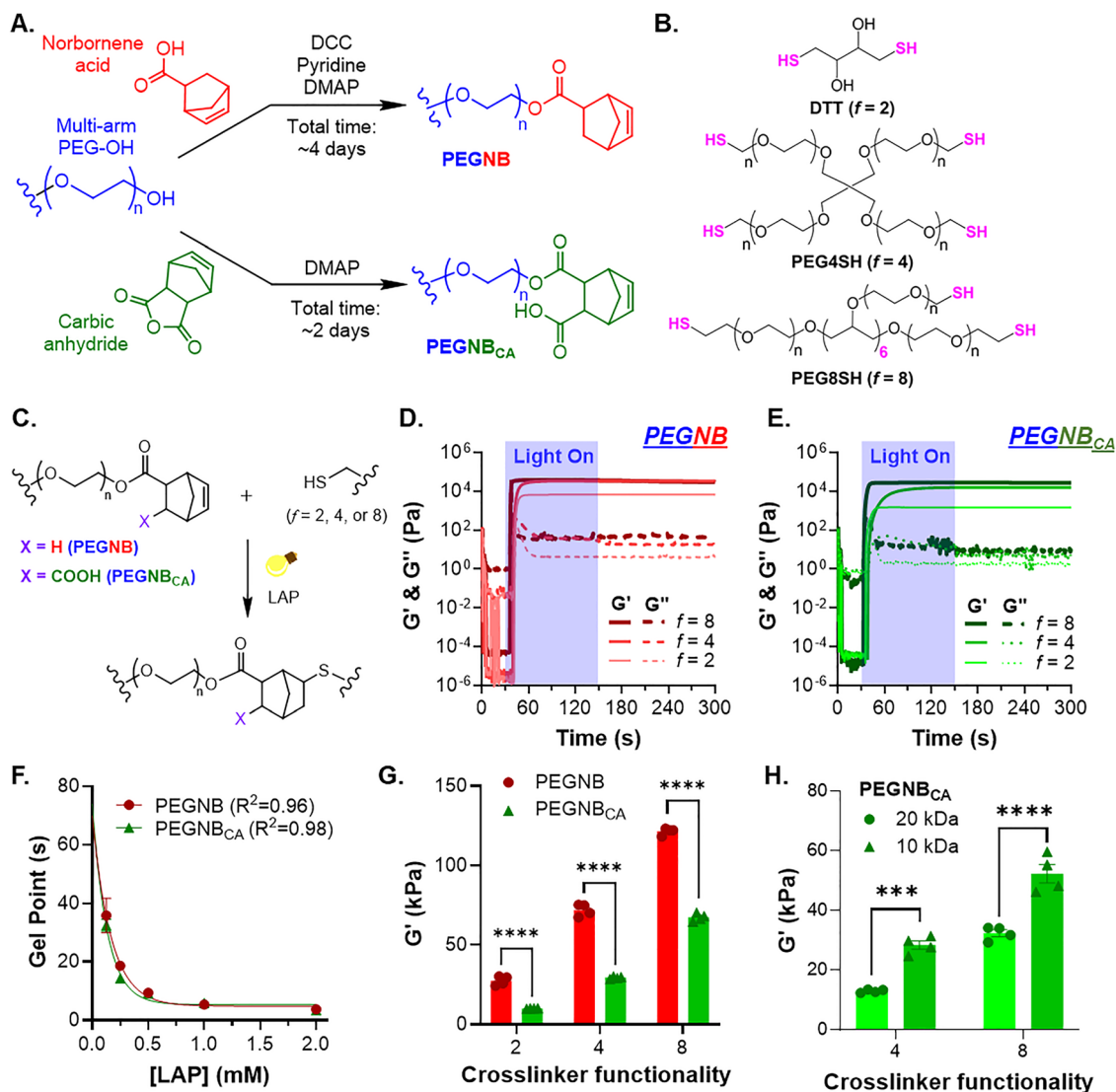


Fig. 1 Photocrosslinking of PEGNB and PEGNB_{CA} with different thiol-bearing macromers. (A) Schematics of PEGNB and PEGNB_{CA} synthesis. (B) Chemical structures of thiol-bearing crosslinkers with different functionalities (2, 4, and 8 for DTT, PEG4SH, and PEG8SH, respectively). (C) Schematic of light and radical-mediated thiol-norbornene photopolymerization. (D) and (E) *In situ* photorheology of gelation using (D) PEGNB or (E) PEGNB_{CA} (both at 5 wt%) with different thiol crosslinkers at a stoichiometric ratio of thiol to norbornene under 365 nm light at 2 mW cm⁻². (F) Effect of LAP concentration on gel points, which were identified from *in situ* photorheometry using 5 wt% PEGNB or PEGNB_{CA} with PEG4SH at a stoichiometric ratio (*R*) of thiol and norbornene under 365 nm light at 3 mW cm⁻². Symbols represent experimental data; curves represent one-phase exponential decay fitting. (G) Initial elastic shear modulus of 5 wt% PEGNB or PEGNB_{CA} crosslinked with different thiol crosslinkers at *R* = 1. All PEGNB variants in (D)–(G) were 8-arm and 20 kDa. (H) Initial elastic shear modulus of 5 wt% PEGNB_{CA} (8-arm, 10 kDa or 20 kDa) crosslinked with either PEG4SH or PEG8SH at *R* = 1.

and ~5 kPa after 5, 10, and 20 minutes, respectively (Fig. S6). This could be explained by the multi-step process of HRP-initiated gelation, where HRP self-oxidation produced endogenous H₂O₂ to catalyze the generation of thyl radicals from thiol-crosslinkers that eventually reacted with PEGNB_{CA}.²⁶ In the absence of exogenous H₂O₂, gelation could be significantly accelerated by increasing the HRP concentration to 1 kU mL⁻¹ (Fig. 2(C) and (D)).²⁶

While HRP alone at high concentration (*e.g.*, 1 kU mL⁻¹) could induce rapid thiol-norbornene gelation of PEGNB_{CA} (gel point ~0.5 minute. Fig. 2(D)), the high enzyme concentration is not desirable due to cost and cytotoxicity concerns. As

addition of H₂O₂ has been shown to drastically accelerate HRP-mediated crosslinking of phenol-rich polymers^{32,33} and thiol-norbornene hydrogels,^{23,26} we reduce the HRP concentration to 10 U mL⁻¹ while adding a small amount of H₂O₂ (25 to 75 μM). At a low HRP concentration of 10 U mL⁻¹ and 25 μM H₂O₂, PEGNB_{CA} hydrogel crosslinking occurred in 12.5 minutes (Fig. 2(E) and Fig. S7). However, increasing H₂O₂ concentration led to significant acceleration of gelation, with a gel point of under 0.8 and 0.1 minute for 50 μM and 75 μM H₂O₂, respectively. Additionally, enzymatically crosslinked PEGNB_{CA} hydrogels could be fabricated to exhibit high elastic moduli, from 20 kPa to nearly 100 kPa (Fig. 2(F)).



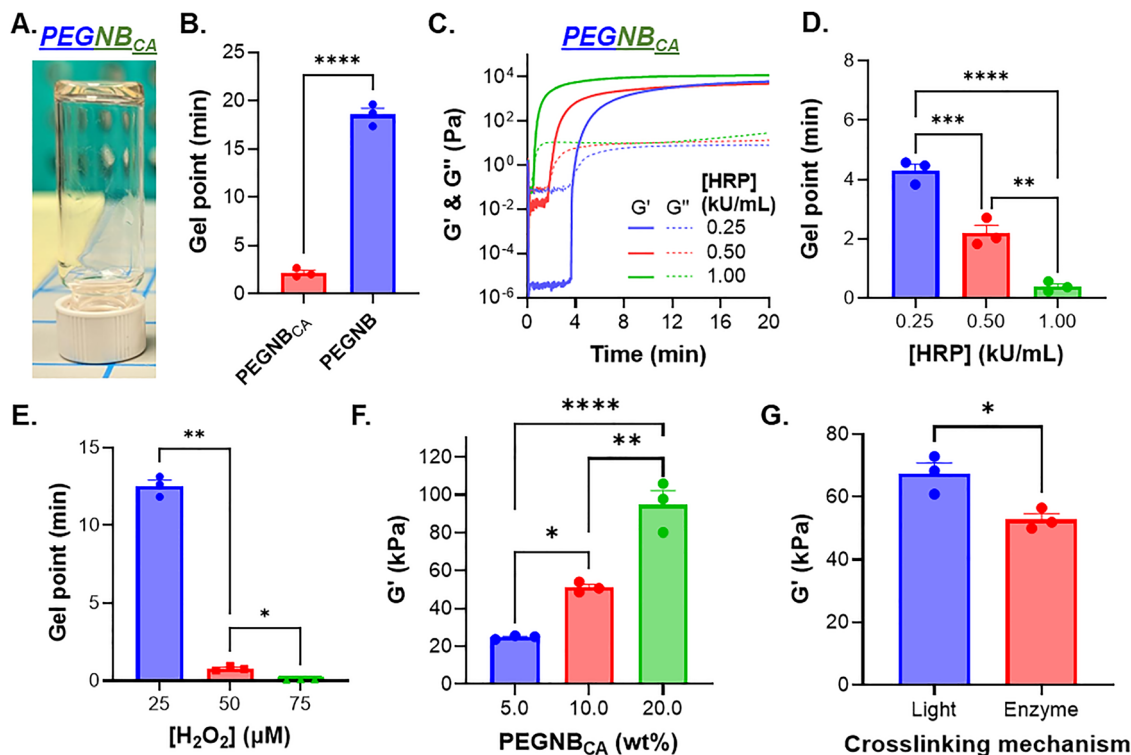


Fig. 2 Enzymatic crosslinking of PEGNB_{CA} hydrogels. (A) Picture of an inverted vial containing a gel formed by 5 wt% 8-arm PEGNB_{CA} (10 kDa), PEG8SH (at $R = 1$), and 0.5 kU mL^{-1} HRP (no exogenous H_2O_2). (B) Gel point derived from *in situ* rheometry data shown in Fig. S6A. (C) *In situ* rheometry of enzymatic crosslinking of 5 wt% PEGNB_{CA} (8-arm, 20 kDa) under different concentrations of HRP with no exogenous H_2O_2 . (D) Gel points identified from Fig. 2(C). (E) Effect of exogenous H_2O_2 concentration on gel points of PEGNB_{CA} gels crosslinked by 10 U mL^{-1} HRP. (F) Effect of the PEGNB_{CA} (8-arm, 20 kDa) concentration of hydrogel moduli. Hydrogels were crosslinked by PEG8SH at $R = 1$ with 20 U mL^{-1} HRP and $0.1 \text{ mM H}_2\text{O}_2$. (G) Effect of the crosslinking mechanism on moduli 10 wt% PEGNB_{CA} hydrogels (8-arm, 20 kDa). Hydrogels were crosslinked by PEG8SH at $R = 1$ through either light-mediated (2 mM LAP , 20 mW cm^{-2} at 365 nm) or the enzymatic reaction (20 U mL^{-1} HRP and $0.1 \text{ mM H}_2\text{O}_2$).

Interestingly, enzymatically crosslinked PEGNB_{CA} hydrogels were softer than their light-crosslinked equivalents (Fig. 2(G)). This was likely due to lower gel fraction (~ 0.8) of the enzymatically crosslinked hydrogels compared with the photopolymerized counterparts (~ 0.98 , Fig. S8). Of note, a gel fraction of 0.8 (*i.e.*, 80% of polymer chains participated in the crosslinking) was still high but nonetheless creates room for improvement in the future. It is also worth noting that both HRP and H_2O_2 were added at concentrations well below what were used previously for thiol–norbornene hydrogel crosslinking.^{23,26} When comparing hydrogels formed by the same HRP-mediated crosslinking, PEGNB_{CA} gelation was more effective than PEGNB (Fig. 2(B)). It is likely that the additional carboxylic acid on PEGNB_{CA} decreased the local pH value around the norbornene groups, creating a slightly acidic local environment that enhanced HRP catalytic activity, which has been shown to be optimum at around pH 6.5.³⁴

Hydrolytic degradation of PEGNB_{CA} hydrogels – effects of pH, temperature, and crosslinking methods

Prior work has demonstrated accelerated hydrolytic degradation of PEGNB_{CA} thiol–norbornene hydrogels compared with their PEGNB counterparts (Fig. 3(A)).¹⁹ However, no detailed characterization was conducted to evaluate the factors affecting

hydrolytic degradation of PEGNB_{CA} hydrogels. In this work, we compared the hydrolytic degradation of PEGNB and PEGNB_{CA} hydrogels in PBS of various pH values – 3 (acidic), 7.4 (physiological), or 12 (basic). Prior to degradation, G'_0 values of all hydrogels were measured and the ratio of G' at any given time over G'_0 was used as a measure of hydrogel degradation. We found that, at pH 12, PEGNB hydrogels degraded rapidly, with complete degradation occurring within 1.5 hours with a hydrolysis reaction constant of 195.3 d^{-1} (Fig. 3(B) and Table S1).³⁵ In contrast, much slower hydrolysis was observed in PEGNB hydrogels incubated in pH 7.4 or pH 3 buffer solutions, with approximately 40% reduction of their initial moduli over 28-day and a hydrolysis reaction constant of 0.01636 d^{-1} at pH 7.4 and 0.01755 at pH 3 (Fig. 3(B) and Table S1). These results aligned with previous finding that thiol–norbornene hydrogels crosslinked by PEGNB were highly susceptible to enhanced hydrolytic degradation in basic solution (*e.g.*, pH 12).^{19,35} Hydrogel degradation was caused by hydrolysis of ester bonds connecting the PEG backbone and the norbornene group, which is known to be accelerated by base-catalyzed nucleophilic acyl substitution of a hydroxide ion ($-\text{OH}$) to the ester's carbonyl carbon. This reaction creates a tetrahedral intermediate that breaks down immediately, releasing an alcohol group and a carboxylic acid group. Interestingly, the equivalent PEGNB_{CA} hydrogels all underwent complete



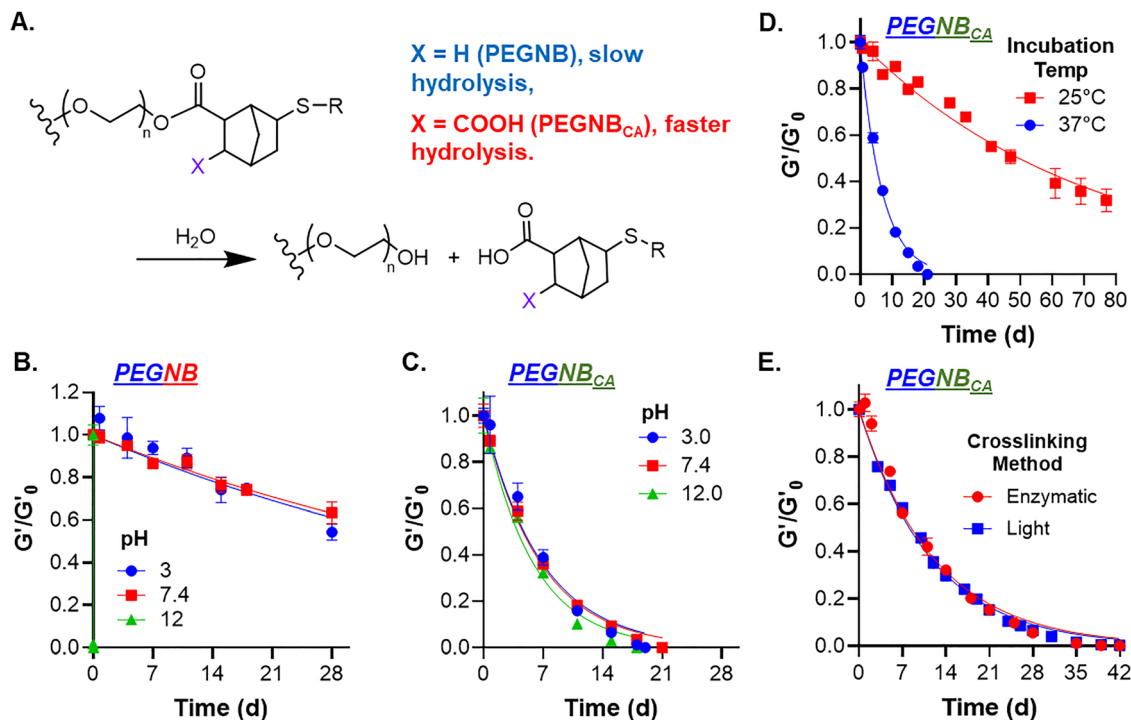


Fig. 3 Hydrolytic degradation of PEGNB_{CA} hydrogels. (A) Reaction schematic of PEGNB or PEGNB_{CA} crosslinked with the thiol macromer undergoing hydrolysis. (B) and (C) Changes in normalized G' of 5 wt% (B) PEGNB or (C) PEGNB_{CA} (8-arm, 20 kDa) crosslinked with PEG4SH at $R = 1$ incubated with PBS at different pH levels. (D) Changes in normalized G' of 5 wt% PEGNB_{CA} (8-arm, 20 kDa) crosslinked with PEG4SH at $R = 1$ incubated with pH 7.4 PBS at 25 °C or 37 °C over time. (E) Changes in normalized G' of 10 wt% PEGNB_{CA} (8-arm, 20 kDa) crosslinked with PEG8SH at $R = 1$. Light based crosslinking occurred using 2 mM LAP with exposure time set at 2 minutes at 20 mW cm⁻². Enzymatic crosslinking occurred in the presence of 20 U mL⁻¹ of HRP and 0.1 mM H₂O₂. Symbols represent experimental data; curves represent one-phase exponential decay fitting.

degradation around 21 days, independent of the pH level in which the hydrogels were incubated (Fig. 3(C) and Table S2). PEGNB_{CA} contains an extra carboxylic acid group, which may provide additional buffering effects to reduce the impact of base-catalyzed hydrolysis, leading to pH-independent degradation kinetics.

Next, the effect of solution temperature (25 °C vs. 37 °C) on the rate of degradation was evaluated. At 37 °C, PEGNB_{CA} hydrogels underwent complete degradation after 21 days (Fig. 3(D)). Degradation was slower at 25 °C, with only about 20% drop in initial elastic moduli over the same period, and complete gel degradation did not occur before ending the study at day-80 (Fig. 3(D)). When fitted with one phase decay fitting, we observed that the derived $k_{\text{hydrolysis}}$ constant was 10 times slower at 25 °C than at 37 °C (Table S3). Previous studies have shown that free radical polymerized PEGDA hydrogels underwent enhanced hydrolytic degradation at higher temperatures, with the reaction/degradation rate described by the classical Arrhenius equation.³⁶ Our results showed that PEGNB_{CA} hydrogels were much more sensitive to temperature change with regard to hydrolysis kinetics than what was previously observed in PEGDA hydrogels.³⁶ The higher sensitivity could result from lower network connectivity at crosslinking sites for step-growth polymerized hydrogels compared to hydrogels crosslinked *via* chain growth polymerization.³⁷

Finally, the effect of the crosslinking method (*i.e.*, photopolymerization or enzymatic crosslinking) on PEGNB_{CA}

hydrogel degradation was compared. PEGNB_{CA} hydrogels were crosslinked with PEG8SH either through LAP-mediated photopolymerization (2 mM LAP with 2-minute light exposure of 365 nm light at 20 mW cm⁻²) or HRP-mediated enzymatic crosslinking (20 U mL⁻¹ HRP and 0.1 mM H₂O₂ reacted at 37 °C). The ratio of G' at any given time over G'_0 was used as a measure of hydrogel degradation so the difference in initial hydrogel crosslinking was not factored into the degradation analysis. Regardless of the crosslinking method, PEGNB_{CA} hydrogels from both groups had nearly identical hydrolysis kinetics and completely degraded after approximately 42 days (Fig. 3(E) and Table S4). This was most likely because the hydrogels were still crosslinked *via* the same thioether bond regardless of the mechanism of initiation.

Hydrolytic degradation of PEGNB_{CA} hydrogels – effects of macromer parameters

As temperature, but not pH nor the crosslinking method, plays a prominent role in dictating the hydrolysis kinetics of PEGNB_{CA} thiol–norbornene hydrogels, all subsequent degradation studies were performed using photopolymerized hydrogels kept at 37 °C and pH 7.4 PBS. Prior work on thiol–norbornene and tetrazine–norbornene PEG-based hydrogels showed that gels crosslinked by a higher macromer content degraded slower.^{21,22} In order to evaluate the effect of the macromer



content on hydrolytic degradation, PEGNB_{CA} hydrogels were formulated into three macromer weight percentages (5 wt%, 10 wt%, and 20 wt%) and crosslinked by thiol-bearing macromers with different functionalities ($f = 2, 4, \text{ and } 8$).¹⁵ Hydrogels were substantially stiffer when crosslinked with higher macromer contents and with higher crosslinker functionality (Fig. S9). The moduli of these PEGNB_{CA} hydrogels spanned across a wide range of physiologically relevant range ($G' \sim 2 \text{ kPa}$ to $\sim 120 \text{ kPa}$).³⁸ When bi-functional DTT was used as the crosslinker, all hydrogels had similarly high gel fraction (> 0.95 , Fig. S10A), as well as comparable mass swelling ratio (Fig. S10B) and mesh size (Fig. S10C). For PEG-based thiol crosslinkers (PEG4SH and PEG8SH), all hydrogels still exhibited high gel fraction (> 0.95 , Fig. S11A), but there was an inverse trend between PEGNB_{CA} weight content and mass swelling ratios (Fig. S11B) and calculated mesh size (Fig. S11C). The differences in swelling and mesh size were likely caused by increased water infiltration in the hydrogels at higher content of PEG-based thiol-crosslinkers. Interestingly, even with these differences, PEGNB_{CA} hydrogels degraded at similar rates independent of the macromer content for all three thiol crosslinkers (Fig. 4(A)). Furthermore, the degradation of PEGNB_{CA} hydrogels

followed pseudo-first order kinetics and displayed high degree fitting to exponential decay (Fig. 4(A)).^{19,39} Higher crosslinker functionality drastically delayed hydrolysis kinetics (Fig. 4(A) and Table S5). For example, at 5 wt% PEGNB_{CA} crosslinked with DTT, PEG4SH, or PEG8SH at $R = 1$, the $k_{\text{hydrolysis}}$ values were 0.3874 d^{-1} , 0.1812 d^{-1} , and 0.07567 d^{-1} , respectively (Table S5), indicating that adjusting crosslinker functionality, rather than the macromer content, would be a more effective way of tuning degradation of these hydrogels. As a comparison, we evaluated the degradation of conventional PEGNB hydrogels crosslinked with DTT, PEG4SH, or PEG8SH *via* tracking their moduli (Fig. S12A). As anticipated, PEGNB hydrogels degraded substantially slower than their PEGNB_{CA} counterpart but generally displayed the same pseudo-first-order degradation kinetics, although all gels remained intact after 200 days. Similar to PEGNB_{CA} gels, the degradation of PEGNB gels was faster when crosslinked by DTT or PEG4SH (Fig. S12B).

We further explored other design parameters that may impact hydrolytic degradation time, such as the stoichiometric ratio of thiol-to-norbornene (*i.e.*, $R = 0.6$ to 1). In general, hydrogels crosslinked with lower R values were softer (Fig. S13A) and degraded slightly faster (Fig. S13B and C). Another parameter

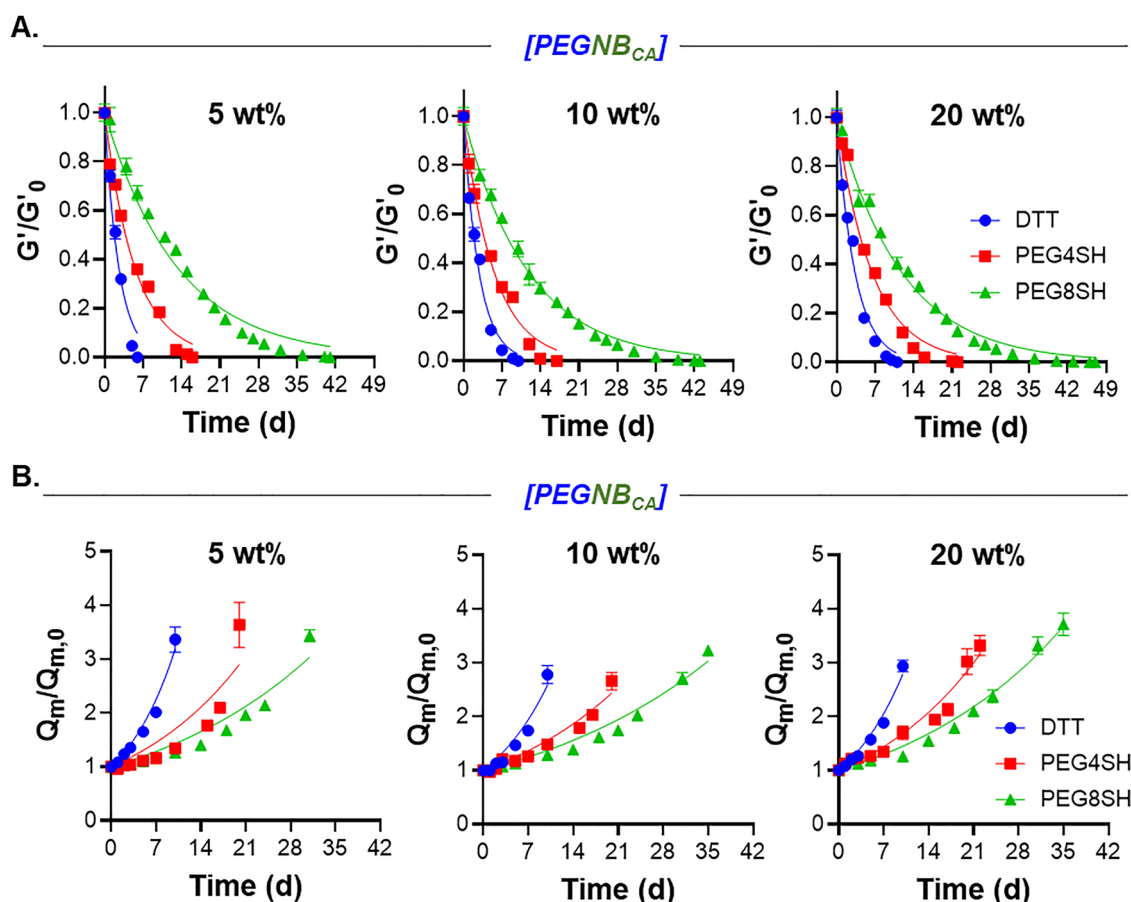


Fig. 4 Effect of the macromer content and thiol-crosslinker functionality on hydrolytic degradation of PEGNB_{CA} hydrogels. (A) Normalized changes in G' or (B) mass swelling ratio over time of PEGNB_{CA} at different macromer concentrations, specifically 5 wt%, 10 wt%, or 20 wt%, crosslinked with either DTT, PEG4SH, or PEG8SH at $R = 1$ incubated in pH 7.4 PBS at 37 °C. Symbols represent experimental data; curves represent one-phase exponential decay fitting.



that may impact hydrolysis kinetics of PEGNB_{CA} hydrogels was the molecular weights of PEGNB_{CA} (e.g., 10 kDa vs. 20 kDa). For 10 kDa PEGNB_{CA} crosslinked by PEG4SH, the hydrolysis kinetics were nearly twice as slow as that of the 20 kDa PEGNB_{CA} counterparts (Fig. S14A), with a complete degradation time of 15 days to 35 days for 20 kDa and 10 kDa PEGNB_{CA}. This could be explained by the difference in crosslinking density produced by the 10 kDa macromer, which had twice the NB molarity to that of the 20 kDa macromer. When crosslinked with PEG8SH, which led to stiffer hydrogels, the difference in the degradation rate was less pronounced (Fig. S14B). Nonetheless, these gels degraded slower than those crosslinked by PEG4SH, with complete degradation time falling between 42 to 50 days.

Hydrolytic degradation of PEGNB_{CA} hydrogels – combinatorial effect of crosslinker functionality and macromer degradability

The combination/blending of fast-degrading PEGNB_{CA} and slow-degrading PEGNB offered an opportunity to engineer

PEG-based hydrogels with programmable hydrolytic degradation. This approach differs from previous chemical strategies that sought to develop norbornene moieties with different hydrolytic susceptibility, which often require advanced chemical synthetic skills.⁴⁰ The crosslinking of blended macromers with different thiol crosslinkers also afforded a simple yet robust method to tune the hydrolytic degradation. To this end, we modularly blended PEGNB_{CA} with PEGNB at different weight ratios (i.e., 4/6, 6/4, 8/2, and 9/1, where the numbers indicate the wt% of PEGNB_{CA} and PEGNB, respectively). For all three thiol crosslinkers (DTT, PEG4SH, and PEG8SH), the higher PEGNB content led to stiffer gels (Fig. 5(A)), agreeing with previous observation that pure PEGNB_{CA} gels were softer than pure PEGNB gels (Fig. 1(G)). However, through modularly blending fast-degrading PEGNB_{CA} with slow-degrading PEGNB, the hydrolytic degradation time was extended from ~49 days (in pure PEGNB_{CA} gels, Fig. 4) to over 150 days and beyond (Fig. 5(B)). Additionally, a wide range of hydrolytic degradation

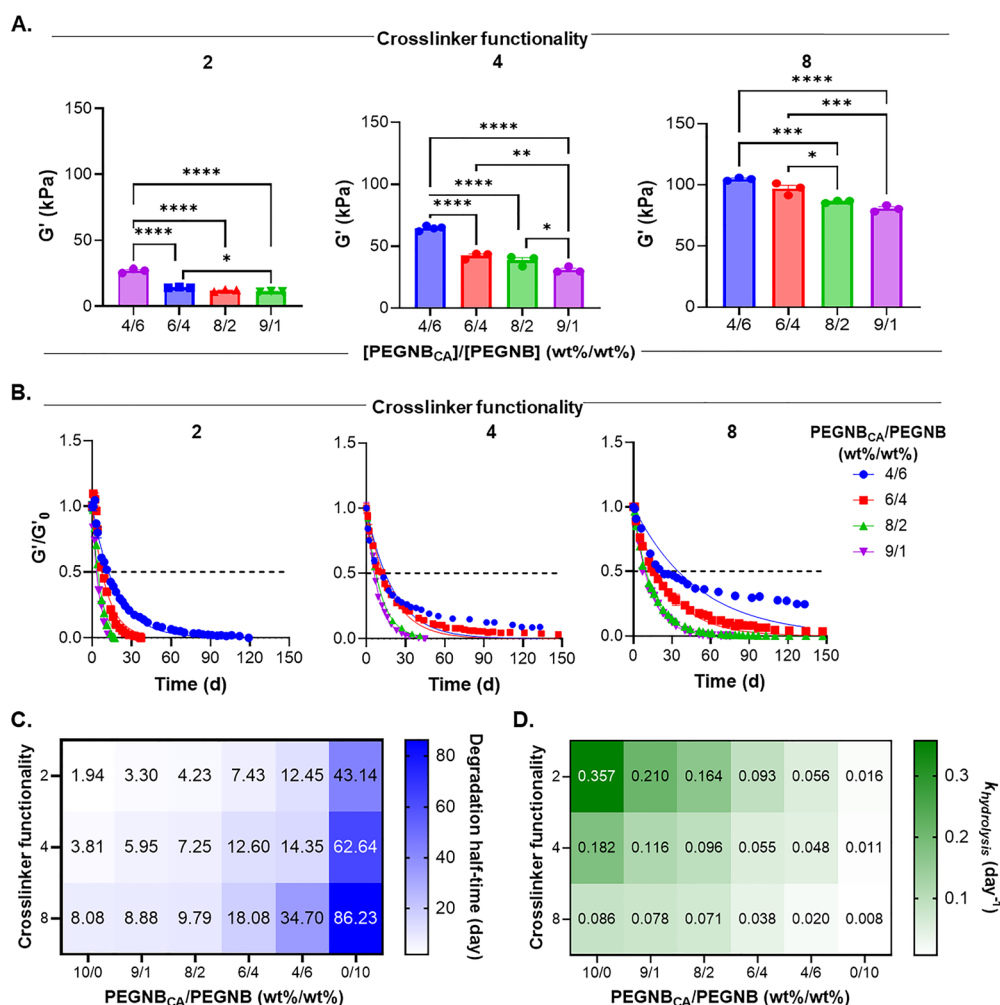


Fig. 5 Blending PEGNB_{CA} and PEGNB together to control the rate of degradation using different thiol crosslinkers. (A) Initial G' and (B) changes in the normalized G' of blended hydrogels crosslinked with DTT, PEG4SH, or PEG8SH. Hydrogels had a fixed total PEGNB/PEGNB_{CA} (8-arm, 20 kDa) concentration of 10 wt% and was crosslinked at $R = 1$. Hydrogels were incubated at 37 °C and swelled in pH 7.4 PBS. Symbols represent experimental data; curves represent one-phase exponential decay fitting. (C) Degradation half-times and (D) $k_{\text{hydrolysis}}$ constants derived from one-phase decay fittings of the changes in G' of the PEGNB_{CA}/PEGNB blended hydrogels over time.



times was achieved through a combinatorial approach of adjusting thiol crosslinker functionality (*i.e.*, $f = 2, 4, \text{ or } 8$) and polymer weight ratio. The degradation half-time, defined as the time required to reach half the initial modulus, varied from less than 2 days to over 86 days (Fig. 5(C) and (D)). Overall, this combinatorial approach of thiol crosslinker functionality and the blended PEGNB_{CA}/PEGNB weight ratio was successful in tuning the hydrolytic degradation over a wide period of time. Future studies could explore the development of generalized mathematical models to predict and validate the effect of various parameters on PEGNB_{CA} hydrogel degradation.⁴¹

Multi-modal controlled release

The high tunability of PEGNB_{CA} hydrogel crosslinking and degradation warrants its use in controlled release applications. The release of hydrogel-encapsulated cargos can be adjusted through many mechanisms, including (1) diffusion-controlled, with release governed by the cargo size; (2) degradation-controlled, with release determined by network connectivity; and (3) diffusion-reaction-controlled, with release controlled by degradation and subsequent diffusion of the molecular tether (Fig. 6(A)). The adaptability of PEGNB_{CA} hydrogels in multi-modal controlled release was first evaluated by diffusion-control release using proteins of three sizes: lysozyme (~14 kDa), BSA (~65 kDa), and BGG (~150 kDa) (Fig. 6(B)). The smallest protein lysozyme diffused out of the 5 wt% PEGNB_{CA} hydrogels rapidly, depleting all releasable protein within hours after the onset of the release study. In contrast, the release of medium-size protein BSA exhibited a bi-phasic profile, with ~30% of burst release in the first 2 hours, followed by a more linear release profile until depleting the releasable protein after 18 days. Finally, the release of the largest protein BGG also exhibited an initial burst of ~20% but no substantial release was detected following the initial burst. The differences in the three release profiles can be explained by the relative sizes of proteins to the mesh size of the hydrogels used (5 wt% 8-arm PEGNBCA + PEG4SH). As shown in Fig. S14B, the calculated mesh sizes of the hydrogels used in the diffusion-controlled release study were between ~15 and ~22 nm. The diameter (2× hydrodynamic radius) of lysozyme, BSA, and BGG was approximately ~4 nm,⁴² ~8 nm,⁴³ and ~10.5 nm,⁴⁴ respectively. It can be reasonably expected that the release would be reduced as the size of diffusants approaches the mesh size of the hydrogel. One interesting phenomenon was that only about 22% BGG was released from the hydrogel at the end of the 18-day release study when the hydrogels were nearly completely degraded (Fig. 4(A)). We reason that some non-specific protein-polymer conjugation might occur between PEGNB_{CA} and BGG during the radical mediated thiol-norbornene gel crosslinking. As BGG is an immunoglobulin containing multiple inter-chain and intra-domain disulfide bonds, radicals generated during hydrogel crosslinking may attack some of these disulfide bonds,⁴⁵ causing its conjugation/immobilization in the thiol-norbornene hydrogel network, hence reducing the amount of total releasable proteins.

To demonstrate degradation-controlled release, we fabricated hydrogels with 10 wt% 8-arm PEGNB_{CA} and PEG8SH, which yielded mesh sizes of ~10 nm to 13 nm (data not shown). We chose FITC-dextran of 70 kDa (dia. ~9 nm) and 150 kDa (dia. ~12 nm) as the model drugs for their larger size and easy fluorescence detection.⁴⁶ As the relative sizes of FITC-dextran and mesh sizes approached one, no significant burst release was found and the cumulative release profiles

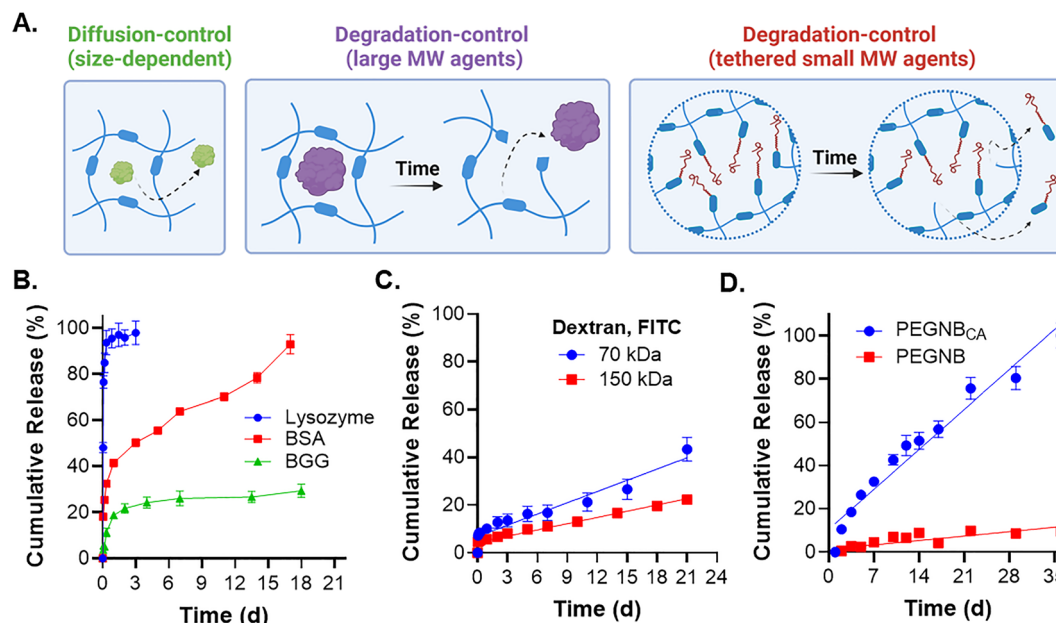


Fig. 6 Controlled release using PEGNB or PEGNB_{CA} thiol-norbornene crosslinked hydrogels. (A) Graphic representing different release strategies using this hydrogel system. (B) Release of lysozyme, BSA, or BGG at 20 mg mL⁻¹ from 5 wt% PEGNB_{CA} (8-arm, 10 kDa) hydrogels. (C) Release of 70 kDa or 150 kDa FITC-dextran from 10 wt% PEGNB_{CA} (8-arm, 10 kDa) hydrogels crosslinked by PEG4SH. (D) Release of PEG-fluorescein-SH (3.4 kDa) conjugated onto 10 wt% PEGNB or PEGNB_{CA} (8-arm, 10 kDa) $R = 0.8$ with PEG8SH.



approached zeroth-order (*i.e.*, release was linear and the release rate was time-independent) (Fig. 6(C)), suggesting a degradation-controlled release.³ We further tested the release of 70 kDa FITC-dextran from hydrogels crosslinked at 2.5 wt%, 5 wt%, and 10 wt% (Fig. S15).³⁹ Since hydrogels crosslinked by lower weight contents had a larger mesh size,^{39,47} higher burst release was observed but these formulations also support higher cumulative release than the highly crosslinked hydrogels.^{3,48}

After demonstrating that PEGNB_{CA} hydrogels could be utilized for controlled release of high molecular weight cargos, we tested if this hydrogel system could be engineered to release smaller molecular weight model drugs. However, since simple encapsulation was ineffective in retaining and controlling the release of small size cargos (lysozyme in Fig. 6(B)), we used 3.4 kDa FITC-PEG-SH as a small size model drug to test whether it could be tethered to the hydrogel network for degradation controlled release.^{9,49} We used the slow-degrading PEGNB hydrogels as a control to evaluate the difference in hydrolysis kinetics on the liberation of the covalently tethered model drug. 3.4 kDa FITC-PEG-SH (dia. <3 nm) was conjugated onto either PEGNB_{CA} or PEGNB during thiol-norbornene hydrogel crosslinking with similar conjugation efficiency (Fig. S16). An off-stoichiometric thiol/norbornene ratio of 0.8 was used to accommodate the conjugation of pendant FITC-PEG-SH. The immobilization of FITC-PEG-SH was visualized and verified *via* fluorescence imaging (Fig. S17A) and intensity quantification (Fig. S17B). FITC-PEG-SH tethered to slow-degrading PEGNB showed low level (<10%) of release after 35 days. In contrast, near-linear release was found when conjugating to the fast-degrading PEGNB_{CA} (Fig. 6(D)). This was a degradation-controlled release as 3.4 kDa FITC-PEG-SH has a hydrodynamic diameter (less than 3 nm per Sigma-Aldrich) much smaller than the mesh size of the hydrogels used here. Its release was essentially determined by the hydrolytic degradation of ester bond linking the drug and the PEG backbone (Fig. 6(A)). The ability of conventional PEGNB to release tethered FITC-PEG-SH was limited due to the slow hydrolysis kinetics of conventional PEGNB. Through these proof-of-concept release studies, we established PEGNB_{CA} hydrogels as a versatile platform for multi-modal controlled release applications. Potential future applications of PEGNB_{CA} hydrogels in drug delivery space include the formulation of highly crosslinked hydrogels with a tunable hydrolysis rate (*via* altering the PEG molecular weight or architecture) for degradation-controlled release of large proteins/antibodies. On the other hand, small molecules can be released from highly swollen PEGNB_{CA} hydrogels *via* covalent tethering as long as the drug contains the free thiol group. Finally, as shown in our previous work, hydrogels crosslinked by PEGNB_{CA} were highly cytocompatible for even highly sensitive induced pluripotent stem cells,^{19,21,22,50} enabling the design of cell-laden hydrogels with controlled release capability to guide stem cell morphogenesis.

Conclusions

In summary, we demonstrated that PEGNB_{CA} supported rapid gelation with thiol-bearing crosslinkers through the light- or

enzyme-mediated thiol-norbornene click reaction. We discovered that the hydrolytic degradation of PEGNB_{CA} hydrogels was pH-independent but temperature-dependent, with higher temperatures accelerating hydrolysis. We systematically characterized the hydrolytic degradation of PEGNB_{CA} hydrogels and developed a simple PEGNB_{CA}/PEGNB blending method to tune the degradation without going through additional chemical synthesis. Finally, this hydrogel system was utilized for multi-modal release of model cargos with different sizes and loading methods (*i.e.*, diffusion-controlled, degradation-controlled release of large molecules, and degradation-controlled release of small tethered molecules). Due to the highly tunable hydrolysis kinetics and the ability to release drug cargo in a controlled release manner, we believe that this hydrogel system will be valuable in the fields of tissue engineering and drug delivery.

Conflicts of interest

There are no conflicts to declare.

Data availability

The data supporting this article have been included as part of the supplementary information (SI). Supplementary information includes additional methods, supporting Fig. S1–S17, supporting Tables S1–S5, and additional references. See DOI: <https://doi.org/10.1039/d5tb01524c>.

Acknowledgements

This work was supported in part by the National Institutes of Health (R01DK127436 to CCL) and the National Science Foundation (NSF GRFP award number: 2141416 to NHD).

References

- 1 C. C. Lin and K. S. Anseth, *Pharm. Res.*, 2009, **26**, 631–643.
- 2 R. Gharios, R. M. Francis and C. A. DeForest, *Matter*, 2023, **6**, 4195–4244.
- 3 C. C. Lin and A. T. Metters, *Adv. Drug Delivery Rev.*, 2006, **58**, 1379–1408.
- 4 A. S. Sawhney and J. A. Hubbell, *J. Biomed. Mater. Res.*, 1990, **24**, 1397–1411.
- 5 A. Metters and J. Hubbell, *Biomacromolecules*, 2005, **6**, 290–301.
- 6 S. C. Rizzi and J. A. Hubbell, *Biomacromolecules*, 2005, **6**, 1226–1238.
- 7 P. van de Wetering, A. T. Metters, R. G. Schoenmakers and J. A. Hubbell, *J. Controlled Release*, 2005, **102**, 619–627.
- 8 S. C. Rizzi, M. Ehrbar, S. Halstenberg, G. P. Raeber, H. G. Schmoekel, H. Hagenmuller, R. Muller, F. E. Weber and J. A. Hubbell, *Biomacromolecules*, 2006, **7**, 3019–3029.
- 9 L. E. Jansen, L. J. Negron-Pineiro, S. Galarza and S. R. Peyton, *Acta Biomater.*, 2018, **70**, 120–128.



- 10 A. Mora-Boza, Z. Ahmedin and A. J. Garcia, *J. Biomed. Mater. Res., Part A*, 2024, **112**, 1265–1275.
- 11 N. M. Shah, M. D. Pool and A. T. Metters, *Biomacromolecules*, 2006, **7**, 3171–3177.
- 12 Y. Hao, H. Shih, Z. Munoz, A. Kemp and C. C. Lin, *Acta Biomater.*, 2014, **10**, 104–114.
- 13 M. R. Arkenberg, H. D. Nguyen and C. C. Lin, *J. Mater. Chem. B*, 2020, **8**, 7835–7855.
- 14 B. D. Fairbanks, M. P. Schwartz, A. E. Halevi, C. R. Nuttelman, C. N. Bowman and K. S. Anseth, *Adv. Mater.*, 2009, **21**, 5005–5010.
- 15 H. Shih and C. C. Lin, *Biomacromolecules*, 2012, **13**, 2003–2012.
- 16 A. Raza and C. C. Lin, *Macromol. Biosci.*, 2013, **13**, 1048–1058.
- 17 M. S. Rehmann, A. C. Garibian and A. M. Kloxin, *Macromol. Symp.*, 2013, **329**, 58–65.
- 18 C. C. Lin, A. Raza and H. Shih, *Biomaterials*, 2011, **32**, 9685–9695.
- 19 F. Y. Lin and C. C. Lin, *ACS Macro Lett.*, 2021, **10**, 341–345.
- 20 Z. Jiang, F. Y. Lin, K. Jiang, H. Nguyen, C. Y. Chang and C. C. Lin, *Biomater. Adv.*, 2022, **134**, 112712.
- 21 N. H. Dimmitt and C. C. Lin, *Macromolecules*, 2024, **57**, 1556–1568.
- 22 N. H. Dimmitt, M. R. Arkenberg, M. M. de Lima Perini, J. Li and C. C. Lin, *ACS Biomater. Sci. Eng.*, 2022, **8**, 4262–4273.
- 23 H. D. Nguyen, H. Y. Liu, B. N. Hudson and C. C. Lin, *ACS Biomater. Sci. Eng.*, 2019, **5**, 1247–1256.
- 24 Y. Qi, F. Wang, J. Liu, C. Wang and Y. Liu, *Int. J. Biol. Macromol.*, 2025, **311**, 143379.
- 25 F. Lee, K. H. Bae and M. Kurisawa, *Biomed. Mater.*, 2015, **11**, 014101.
- 26 M. H. Kim and C. C. Lin, *Biomed. Mater.*, 2021, **16**, 045027.
- 27 B. D. Fairbanks, M. P. Schwartz, C. N. Bowman and K. S. Anseth, *Biomaterials*, 2009, **30**, 6702–6707.
- 28 C. Y. Chang, H. C. Johnson, O. Babb, M. L. Fishel and C. C. Lin, *Acta Biomater.*, 2021, **130**, 161–171.
- 29 M. Shibayama, *Soft Matter*, 2012, **8**, 8030–8038.
- 30 T. Sakai, Y. Akagi, T. Matsunaga, M. Kurakazu, U. I. Chung and M. Shibayama, *Macromol. Rapid Commun.*, 2010, **31**, 1954–1959.
- 31 J. R. Clegg, K. Adebowale, Z. Zhao and S. Mitragotri, *Bioeng. Transl. Med.*, 2024, **9**, e10680.
- 32 D. L. Lefkowitz, K. Mills, A. Castro and S. S. Lefkowitz, *J. Leukocyte Biol.*, 1991, **50**, 615–623.
- 33 J. J. Roberts, P. Naudiyal, K. S. Lim, L. A. Poole-Warren and P. J. Martens, *Biomater. Res.*, 2016, **20**, 30.
- 34 A. J. AL-Sa'ady, M. H. A. Al-Bahrani and G. M. Aziz, *Int. J. Curr. Microbiol. Appl. Sci.*, 2018, **7**, 328–339.
- 35 S. E. Holt, A. Rakoski, F. Jivan, L. M. Perez and D. L. Alge, *Macromol. Rapid Commun.*, 2020, **41**, e2000287.
- 36 G. J. Rodriguez-Rivera, M. Green, V. Shah, K. Leyendecker and E. Cosgriff-Hernandez, *J. Biomed. Mater. Res., Part A*, 2024, **112**, 1200–1212.
- 37 M. W. Tibbitt, A. M. Kloxin, L. Sawicki and K. S. Anseth, *Macromolecules*, 2013, **46**, 2785–2792.
- 38 T. Su, M. Xu, F. Lu and Q. Chang, *RSC Adv.*, 2022, **12**, 24501–24510.
- 39 C. E. Ziegler, M. Graf, M. Nagaoka, H. Lehr and A. M. Goepferich, *Biomacromolecules*, 2021, **22**, 3223–3236.
- 40 G. R. Sama, M. N. Arguien, T. E. Hoffman, B. D. Fairbanks, M. Trujilo-Lemon, S. Keyser, K. S. Anseth, S. L. Spencer and C. N. Bowman, *Biomacromolecules*, 2025, **26**, 1850–1859.
- 41 R. Das and D. Kundu, *Comput. Mater. Sci.*, 2025, **247**, 113516.
- 42 Y. Zhang; E. Farrell; D. Mankiewicz and Z. Weiner, *Brookhaven Instruments Application Library*, 2019.
- 43 A. Hawe, W. L. Hulse, W. Jiskoot and R. T. Forbes, *Pharm. Res.*, 2011, **28**, 2302–2310.
- 44 M. Nag, D. Das, D. Bandyopadhyay and S. Basak, *Phys. Chem. Chem. Phys.*, 2015, **17**, 19139–19148.
- 45 B. D. Fairbanks, S. P. Singh, C. N. Bowman and K. S. Anseth, *Macromolecules*, 2011, **44**, 2444–2450.
- 46 M. C. Branco, D. J. Pochan, N. J. Wagner and J. P. Schneider, *Biomaterials*, 2009, **30**, 1339–1347.
- 47 B. Henry, M. Cheema and S. Davis, *Int. J. Pharm.*, 1991, **73**, 81–88.
- 48 E. Axpe, D. Chan, G. S. Offeddu, Y. Chang, D. Merida, H. L. Hernandez and E. A. Appel, *Macromolecules*, 2019, **52**, 6889–6897.
- 49 A. Metters, K. Anseth and C. Bowman, *Polymer*, 2000, **41**, 3993–4004.
- 50 N. H. Dimmitt and C. C. Lin, *Adv. Mater. Interfaces*, 2025, 2400952.

